



## Article

# Wavelength Calibration for the LIBS Spectra of the Zhurong Mars Rover

Yizhong Zhang <sup>1,2,\*</sup>, Xin Ren <sup>1,2,\*</sup>, Zhaopeng Chen <sup>1,2</sup>, Wangli Chen <sup>1</sup>, Zhenqiang Zhang <sup>3</sup>, Xiangfeng Liu <sup>3</sup>, Weiming Xu <sup>3</sup>, Jianjun Liu <sup>1,2</sup> and Chunlai Li <sup>1,2</sup>

<sup>1</sup> Key Laboratory of Lunar and Deep Space Exploration, National Astronomical Observatories, Chinese Academy of Sciences, Beijing 100101, China

<sup>2</sup> School of Astronomy and Space Sciences, University of Chinese Academy of Sciences, Beijing 100049, China

<sup>3</sup> Key Laboratory of Space Active Opto-Electronics Technology, Shanghai Institute of Technical Physics, Chinese Academy of Sciences, Shanghai 200083, China

\* Correspondence: renx@nao.cas.cn

**Abstract:** China's first Mars rover, Zhurong, landed on the southern region of Utopia Planitia, Mars, on 14 May 2021 (UTC). Zhurong is equipped with the Mars Surface Composition Detection Package (MarSCoDe), which analyzes the Martian surface's material composition. Composed of laser-induced breakdown spectroscopy (LIBS), short-wave infrared spectroscopy (SWIR), and a microimaging camera, MarsCoDe can work at a distance of 1.6–7 m to analyze element abundance and the mineralogy of targets on the Martian surface. Analysis shows that the wavelengths of MarSCoDe onboard LIBS spectra acquired within the same probe period will have different degrees of drift, leading to deviation in qualitative and quantitative elemental analysis. This paper finds that the spectrum drift follows a quadratic function relationship with the CCD temperature of the MarSCoDe spectrometer, based on which a wavelength calibration method is established. According to the function, the drift of a certain channel is calculated by the corresponding CCD temperature, and then the wavelength of the spectrum is calibrated by the drift. The accuracy of this calibration method for the position of peak wavelength in the LIBS spectrum can reach about 1/5 of the apparatus spectral width, and the cross-validation analysis using a norite standard sample shows that it is comparable to the wavelength calibration accuracy of the ChemCam onboard data product.

**Keywords:** laser-induced breakdown spectroscopy; wavelength calibration; MarSCoDe



**Citation:** Zhang, Y.; Ren, X.; Chen, Z.; Chen, W.; Zhang, Z.; Liu, X.; Xu, W.; Liu, J.; Li, C. Wavelength Calibration for the LIBS Spectra of the Zhurong Mars Rover. *Remote Sens.* **2023**, *15*, 1494. <https://doi.org/10.3390/rs15061494>

Academic Editor: Jonathan H. Jiang

Received: 23 December 2022

Revised: 20 January 2023

Accepted: 26 January 2023

Published: 8 March 2023



**Copyright:** © 2023 by the authors. Licensee MDPI, Basel, Switzerland. This article is an open access article distributed under the terms and conditions of the Creative Commons Attribution (CC BY) license (<https://creativecommons.org/licenses/by/4.0/>).

## 1. Introduction

Laser-induced breakdown spectroscopy (LIBS) is a rapid analysis technology of material composition. In practice, LIBS works to focus a pulsed laser beam on the surface of the target to be observed. A target material can be broken down by an intense photon flux into a high-temperature plasma, and then use a spectrometer to collect the atomic emission spectrum of the plasma. The element abundance of a target could be obtained by analyzing the spectrum collected [1,2]. Compared with an alpha particle X-ray spectrometer (APXS), X-ray fluorescence (XRF), mass spectrometry (MS), and other material composition analysis methods, LIBS is remote sensing detection, which can probe difficult-to-reach targets. Besides, targets for LIBS observation do not need pretreatment. LIBS can analyze element abundance and mineralogy, especially for light elements, including hydrogen and carbon, which are difficult to analyze by other methods, such as XRF. Through laser ablation, LIBS can remove dust from the target surface and excavate into the target, which provides a window to the composition of the target subsurface [1–3].

Due to these advantages, LIBS technology has been applied to Earth and planetary science research. The ChemCam instrument package on NASA's Curiosity rover is the first planetary science instrument to employ LIBS to determine the compositions of geological samples on another planet [4,5]. Since landing in the Gale crater in 2012, ChemCam has

been used to study the elemental abundance of Martian surface targets, such as Martian soil, sand, dust, and sedimentary and igneous rocks [6–13]. As the successor of ChemCam, SuperCam is mounted on the Perseverance rover [14,15] and landed in the Jezero crater on 19 April 2021. So far, the data product of SuperCam during the first 299 days on Mars has been released and is available at [https://pds-geosciences.wustl.edu/m2020/urn-nasa-pds-mars2020\\_supercam/](https://pds-geosciences.wustl.edu/m2020/urn-nasa-pds-mars2020_supercam/) (8 April 2022).

The LIBS analysis method is derived from atomic emission spectroscopy. Emission peaks with characteristic wavelengths in the spectrum correspond to different elements, which is the basis of chemical analysis by atomic spectroscopy [3]. According to the characteristic wavelength and intensity of the emission peaks in the collected LIBS spectrum, the species and abundance of elements contained in the target could be determined. The accuracy of the wavelength will directly affect the accuracy of the spectral analysis. Therefore, wavelength calibration should be the first step in LIBS analysis. A standard method of calibration is to use a spectral lamp made for specific elements, such as a mercury lamp. These lamps could produce stable and easily identifiable emission peaks with known wavelengths. Based on these peaks, the spectrum can be calibrated. Other sources that could provide stable and characteristic peaks are available as substitutes for spectral lamps [3]. ChemCam finished its wavelength baseline calibration with a titanium plate, also carried as an onboard calibration target. Experience from ChemCam shows that the difference in environmental conditions between Earth and Mars could cause a drift in the wavelength of the LIBS spectrum. The wavelengths of a ChemCam onboard LIBS spectrum are calibrated according to wavelength drifts of titanium spectra relative to that taken in the lab [4,14,16,17].

China's first Mars rover, Zhurong, landed in the southern region of Mars' Utopia Plain on 14 May 2021. The Mars Surface Composition Detection Package (MarSCoDe) onboard Zhurong consists of a LIBS spectrometer, a SWIR spectrometer, and a microimaging camera. Mounted on the left side of the front of the rover, MarSCoDe is expected to provide mineralogy, chemical element abundance, and a detailed image of the Martian soil, rocks, and other targets within the range of 1.7–7 m in front of the rover [18]. A titanium onboard calibration target (referred to as Ti plate) is contained in MarSCoDe calibration targets (MCCT), the onboard spectra of which will be collected according to the demand for correction of drifts in all LIBS spectra during the in situ exploration of LIBS. However, the analysis shows that within the same probe period, the drifts of different target spectra collected by MarSCoDe are inconsistent and cannot be directly calibrated by the drift of the Ti plate relative to the laboratory reference spectrum. In this paper, we analyzed the drift of the Ti plate's onboard spectra relative to the reference spectrum from the lab. We confirmed that the CCD temperature of the MarSCoDe spectrometer is the leading cause of wavelength drift and found that the drift follows a quadratic function with CCD temperature. We established a wavelength correction method for MarSCoDe LIBS based on this function.

## 2. Materials and Methods

### 2.1. MarSCoDe Instrument and Data Description

MarSCoDe, integrating LIBS, SWIR, and a microimaging camera, is the main material composition analysis load of the Zhurong rover. It is used to identify the elemental abundance and mineralogy of the rocks, soil, and other targets on the Martian surface within a distance of 1.7–7 m. MarSCoDe comprises two parts: the part outside the rover, which includes a 2D pointing mirror and optical head, and the part inside the rover, which includes a LIBS spectrometer, short-wave infrared spectrometer, and main control unit. The LIBS laser operates at 1064.4 nm, with a frequency of 1–3 Hz and a laser energy of 23 mJ. The LIBS spectrometer consists of 3 channels, channel 1 (CH1) covering 240–340 nm, channel 2 (CH2) covering 340–540 nm, and channel 3 (CH3) covering 540–850 nm, with spectral FWHM resolutions of 0.19, 0.31, and 0.45 nm, respectively. The spectrometer is a cross-type Czerny–Turner configuration. This optical system can ensure that each channel

has a stable apparatus spectral width, of which CH1, CH2, and CH3 are 0.067, 0.133, and 0.2 nm/pixel, respectively, which ensures a stable relative interval between emission peaks in the collected LIBS spectrum [18]. For onboard calibration of LIBS spectra, MarSCoDe carries 12 standard samples, including basalt, andesite, montmorillonite, nontronite, dolomite, gypsum, K-feldspar, apatite, hypersthene, norite [19], and a Ti plate (TC4KY titanium alloy), mounted at the base of the directional antenna mast, 1.7 m away from the MarSCoDe 2D pointing mirror, among which the Ti plate is used for wavelength calibration of LIBS data because Ti provides multiple stable and emission peaks in all three channels. Details of the structure are shown in Figure 1.

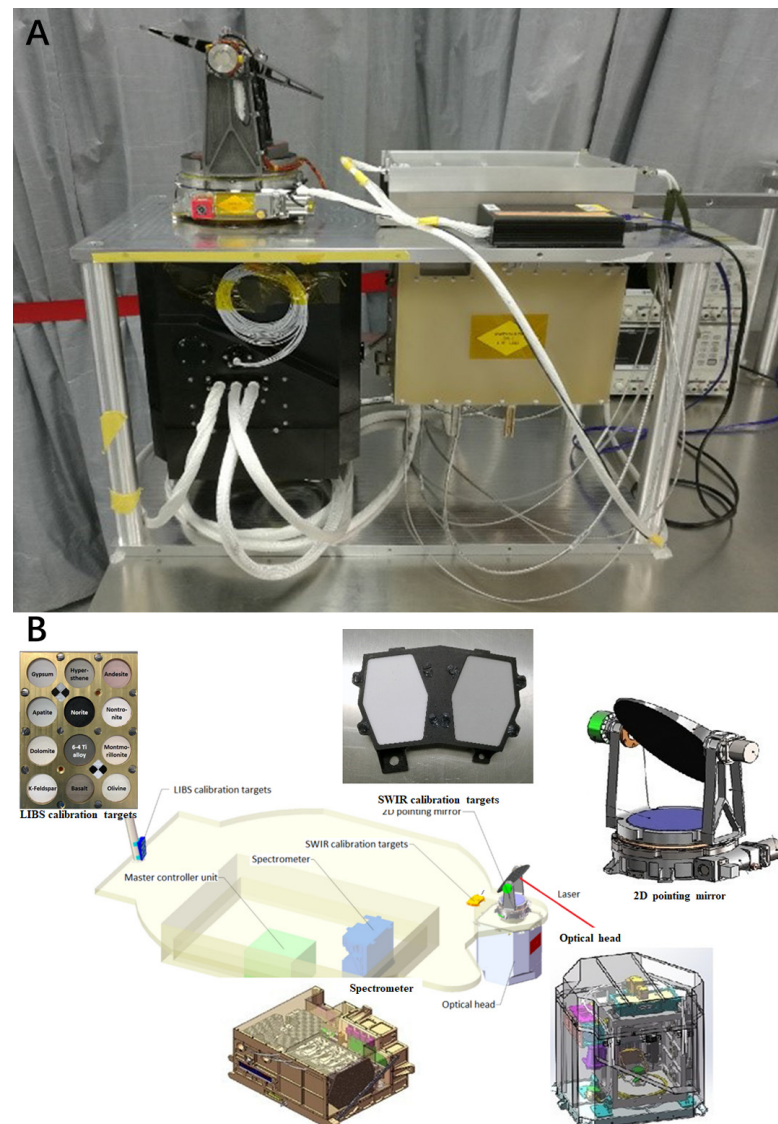


**Figure 1.** Diagram of MarSCoDe: (A) is a picture of a real product taken in the lab, and (B) shows the structural layout of MarSCoDe.

In each probe, MarSCoDe collects LIBS spectra of 2–3 MCCT targets first and then 2 Martian surface targets, and the operating time is within 1 h. While observing a single target, MarSCoDe first emits dozens of pulsed lasers on the target surface for focusing and then emits 60 laser pulses and collects the spectral data of the plasma excited by each pulse. An example of a spectrum of a basalt target is shown in Figure 2.

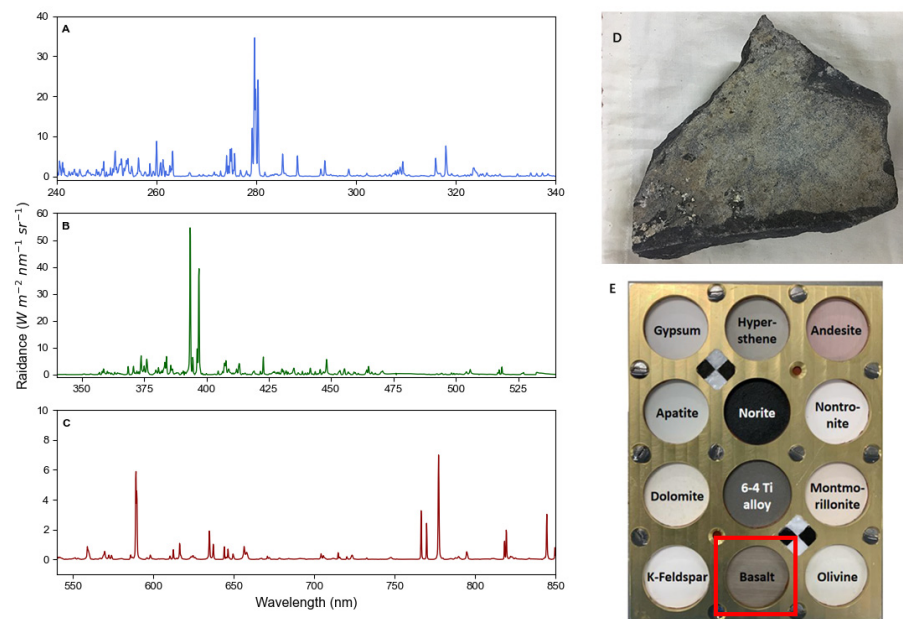


**Figure 2.** The spectrum of the basalt target: (A–C) are the spectrum divided into three channels, (D) is the raw material of the basalt target, and (E) shows the assembled targets.

The MarSCoDe LIBS data consist of radiance values corresponding to 5400 pixels. The baseline calibration of pixel serial number to wavelength is based on spectral lamps, and the pixel–wavelength relationships of the three different channels are calibrated with different quadratic polynomials shown in as follow equations [18]:

$$\text{CH1: } \lambda_i = -8.2182 \times 10^{-7}(x_{1i} + \Delta x_1 + 1.65)^2 + 0.068195(x_{1i} + \Delta x_1 + 1.65) + 223.4469, i = 1 \sim 1800 \quad (1)$$

$$\text{CH2: } \lambda_j = -1.1305 \times 10^{-6}(x_{2j} + \Delta x_2 + 1.23)^2 + 0.13855(x_{2j} + \Delta x_2 + 1.23) + 76.7245, j = 1801 \sim 3600 \quad (2)$$

$$\text{CH3: } \lambda_k = -2.1602 \times 10^{-6}(x_{3k} + \Delta x_3 + 1.41)^2 + 0.22264(x_{3k} + \Delta x_3 + 1.41) - 258.0135, k = 3601 \sim 5400 \quad (3)$$

In the formula,  $\lambda_i$ ,  $\lambda_j$ , and  $\lambda_k$  are the wavelength values (nm) of each pixel after transportation, and  $x_1$ ,  $x_2$ , and  $x_3$  are the pixel serial numbers (pixel) in CH1, CH2, and CH3, respectively.  $\Delta x_1$ ,  $\Delta x_2$ , and  $\Delta x_3$  are average pixel drifts of CH1, CH2, and CH3 of an onboard Ti plate LIBS spectrum to reference spectra from the lab. Reference spectra from the lab were taken on the Ti plate in MCCT by MarSCoDe under simulated Martian atmospheric conditions (atmospheric composition of 1.6% Ar, 2.7% N<sub>2</sub>, 95.7% CO<sub>2</sub>, and pressure of  $700 \pm 50$  Pa). Details of reference spectra from the lab are shown in Table S1 (see Supplementary Materials).

As of 3 September 2021 (Sol 110, the last time MarSCoDe was activated before the solar transit), MarSCoDe has carried out 16 probes. The Ti plate was observed in each probe for wavelength position calibration. This paper used reference spectra from the lab and MarSCoDe onboard LIBS data of the Ti plate collected during Sol 32 to 92 to establish a universal wavelength calibration method for all MarSCoDe LIBS data, including both MCCT standards and Martian surface targets. Moreover, onboard LIBS data of the Ti plate collected on Sol 100, 103, and 110 and of norite collected on Sol 41 and 43 were employed to test the accuracy of the newly established method.

Onboard data were processed in the following steps: (1) averaging the 60-shot LIBS spectra, (2) subtracting the dark background from the averaged spectra, (3) ChemCam-style wavelet denoising [16], (4) converting the relative values of the instrument response to irradiance (only for norite spectra), and (5) asymmetric least squares (ALS) baseline extraction and deduction [20]. The result was a continuous atomic spectrum with white noise and plasma continuum removed from the spectrum and kept pixels on the x-axis of spectra for subsequent calibration. The data processing flow is shown in Figure 3.

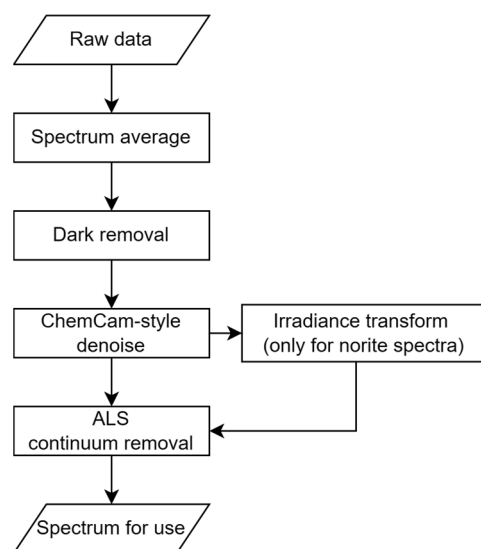


**Figure 3.** Data processing flow.

It should be noted that the range of the mean value of relative standard deviation (RSD) of each pixel in the spectrum of the Sol 32 to 92 Ti plate is 0.01–0.02, and the range of the maximum value of RSD is 0.06–0.33. Spectra present good reproducibility, and very few high RSDs are caused by the weak signal of some pixels. This is the premise of using the average spectrum.

## 2.2. Method for MarSCoDe Wavelength Calibration

The considerable difference between the Martian surface and Earth’s environment, especially the low temperature and air pressure, will inevitably cause the LIBS spectrum to drift relative to that in the ground lab. To correct this drift, MarSCoDe first observes MCCT onboard standards (including Ti plate) in each probe and then observes the Martian surface targets after about 20 min.

In the initial data processing, the wavelength value transported from the pixel of the onboard LIBS spectrum was calculated using Equations (1)–(3) in Section 2.1. The values of  $\Delta x_1$ ,  $\Delta x_2$ , and  $\Delta x_3$  are obtained by matching the spectra of the Ti plate in each probe with reference spectra from the lab, and then they are substituted into Equations (1)–(3) to calculate the wavelength of each pixel. The wavelength thus obtained is initially considered, which could be used for every LIBS spectrum of targets in one probe.

However, since no active thermal control is taken on the MarSCoDe LIBS spectrometer, its operating temperature varies during each probe, which could rise by 5–8 °C until it is turned off. This significantly affects the CCD temperature of each channel whenever at the time MarSCoDe starts operating or takes LIBS on targets, resulting in the drift of the spectral position changing with temperature. The analysis of the spectrum of different targets in one probe shows that the wavelength deviation of the same emission peak between Martian surface targets and MCCT standards in the same probe (due to the different spectral collecting times resulting in the different CCD temperatures) can reach more than 0.3 nm.

In this section, drifts of LIBS data collected by MarSCoDe LIBS on the Ti plate during Sol 32 to 92 at different CCD temperatures relative to reference spectra from the lab were analyzed. Therefore, we determined the relationship between drift in the spectrum and CCD temperature, and a fitting function between the above two was established. Based on this relationship, the wavelength of each pixel in each channel of LIBS can be calibrated accurately.

### 2.2.1. Calibration Peaks and Their Drifts

To obtain drifts at different positions within the channel and to check whether the drift is equal, we selected a series of emission peaks in the LIBS spectra of the Ti plate as

calibration peaks. The emission peaks selected as calibration peaks are easily excited by the laser, have less fluctuation in peak intensity, and are relatively uniformly distributed over the entire spectrum (Figure 4, Table S2 in Supplementary Materials). Tests show that calibration peaks generally have a high signal-to-noise ratio (SNR), and the calibration peak SNR of each channel is greater than 112, 55, and 16, respectively, which can be easily identified from the spectrum.

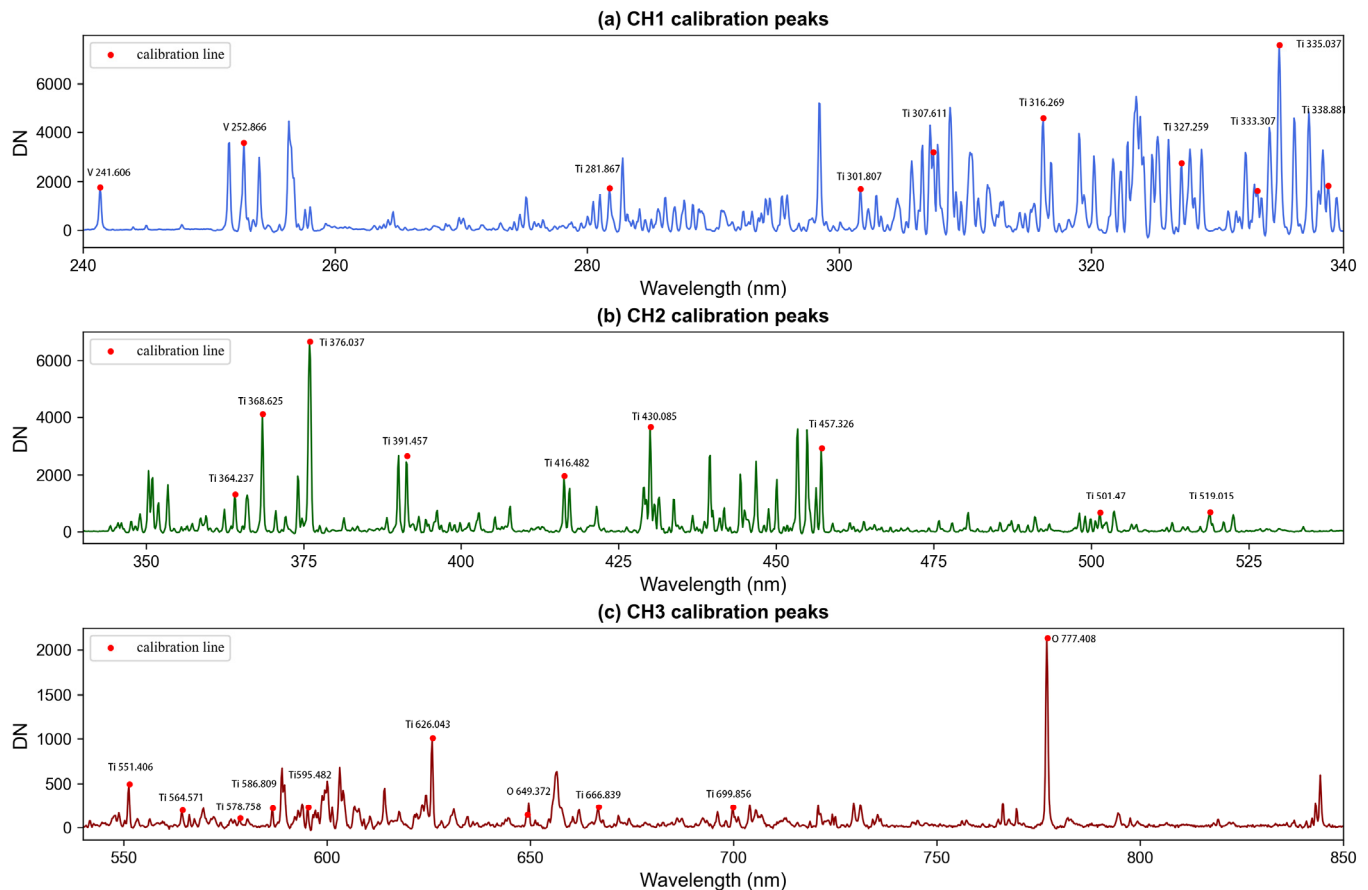


**Figure 4.** Calibration peaks in the titanium LIBS spectrum: (a–c) are calibration peaks in CH1, CH2, and CH3. The Ti spectrum shown above is the Ti calibration target and taken in the ground lab, and the spectral intensity is shown in digital number (DN).

According to the reference spectra from the lab, the spectral drift of the calibration peak in the onboard LIBS spectrum of the Ti plate can be calculated (Table S2). The data show that the onboard spectrum generally drifts to the right (longwave direction) relative to the reference spectra from the lab, and drifts in CH3 are the most significant.

The drift of different calibration peaks within the same channel is basically the same. Table 1 shows that the maximum deviations among drifts of the calibration peaks in CH1, CH2, and CH3 are, respectively, 0.61, 0.34, and 0.61 pixels (transporting to wavelength are 0.041, 0.045, and 0.122 nm), and much smaller than the apparatus spectral width. Moreover, the relative standard deviation (RSD) of calibration peak drifts in most spectra is less than 5%, indicating that drift values in the same channel are statistically uniform, which means that the average drift of calibration peaks in a channel could be considered as the drift of that channel of the Ti plate (see Table 1 average). The excessive RSD of calibration peak drifts in a few spectra is due to a slight average drift, and as an example, Sol 50 CH1 has an average drift of only 0.05 pixels and a standard deviation of 0.12. In addition, the drift among the three channels is only partially consistent, and so is the drift between different Martian days in the same channel (Figure 5).

**Table 1.** Average, standard deviation (SD), relative standard deviation (RSD), and maximum value of the calibration peak drift of each channel, taken from the titanium target LIBS spectrum during Sol 32 to 92 (unit: pixel value).

Channel	Parameter	Sol 32	Sol 41	Sol 43	Sol 45	Sol 47	Sol 50	Sol 58	Sol 65	Sol 69	Sol 79	Sol 87	Sol 92
CH1	Average	2.29	0.37	3.66	0.47	3.74	0.05	4.11	1.61	1.05	1.07	1.15	2.25
	SD	0.15	0.09	0.13	0.09	0.16	0.12	0.18	0.10	0.13	0.13	0.13	0.16
	RSD(%)	6.55	24.32	3.55	19.15	4.28	240.00	4.38	6.21	12.38	12.15	11.30	7.11
	Max delta	0.41	0.22	0.41	0.22	0.51	0.41	0.61	0.31	0.41	0.41	0.41	0.41
CH2	Average	2.40	1.40	3.40	1.56	3.49	1.30	3.86	2.20	1.87	1.90	1.90	2.37
	SD	0.11	0.12	0.11	0.12	0.12	0.12	0.09	0.11	0.08	0.08	0.08	0.11
	RSD(%)	4.58	8.57	3.24	7.69	3.44	9.23	2.33	5.00	4.28	4.21	4.21	4.64
	Max delta	0.29	0.29	0.29	0.34	0.29	0.29	0.25	0.29	0.24	0.25	0.25	0.29
CH3	Average	16.90	13.61	17.59	13.80	17.74	12.77	17.89	16.35	15.70	15.74	15.75	16.73
	SD	0.14	0.09	0.18	0.08	0.08	0.13	0.07	0.14	0.10	0.09	0.13	0.12
	RSD(%)	0.83	0.66	1.02	0.58	0.45	1.02	0.39	0.86	0.64	0.57	0.83	0.72
	Max delta	0.50	0.28	0.61	0.26	0.30	0.37	0.20	0.40	0.29	0.29	0.49	0.39

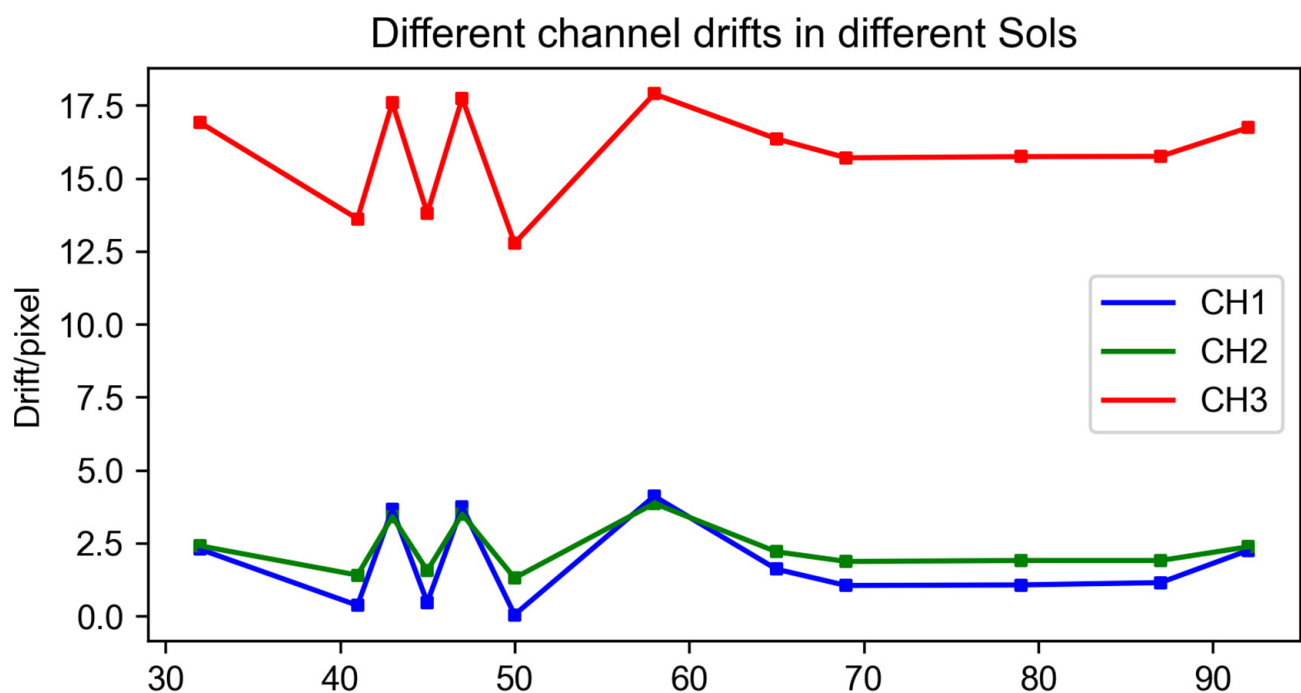


**Figure 5.** Change of the average drift of each channel, taken from the titanium target LIBS spectrum during Sol 32 to 92.

### 2.2.2. Relationship between Calibration Peak Drift and MarSCoDe LIBS CCD Temperature

In the early tests of MarSCoDe, the spectrometer was placed at different ambient temperatures ( $-46$ – $56$  °C) to acquire the spectra of Hg–Ar lamps. The results show that the spectral position of Hg–Ar lamps drifts with temperature, and as the temperature increases, the value of the spectral drift (reference temperature is 20 °C) decreases [18]. In the ground test of ChemCam, the spectral drift also showed a trend of decreasing with the spectrometer's temperature increase. There was an approximately linear relationship between the drift values and the temperature of the body unit of ChemCam. All three spectrometers had the goodness of fit ( $r^2$ ) of 1, 0.94, and 0.97 [4].

The temperature analysis of the spectrometer CCD in MarSCoDe onboard LIBS data shows that the CCD temperature rises with the operating time, which leads to different CCD temperatures at different LIBS collecting times. The comparative analysis of the same emission peaks of different targets (meaning different times) in one probe shows that the wavelength positions of the LIBS data taken later have a smaller drift value, corresponding to a higher CCD temperature.

CCD temperature in LIBS data of the Ti plate taken during Sol 32 to 92 is extracted, then the correlation coefficient of each channel between the CCD temperature and the drift is calculated. CH1, CH2, and CH3 are  $-0.95$ ,  $-0.92$ , and  $-0.99$ , indicating a highly negative correlation between CCD temperature and drift (see Figure 6), which is consistent with ground test results of MarSCoDe and similar to that of ChemCam.

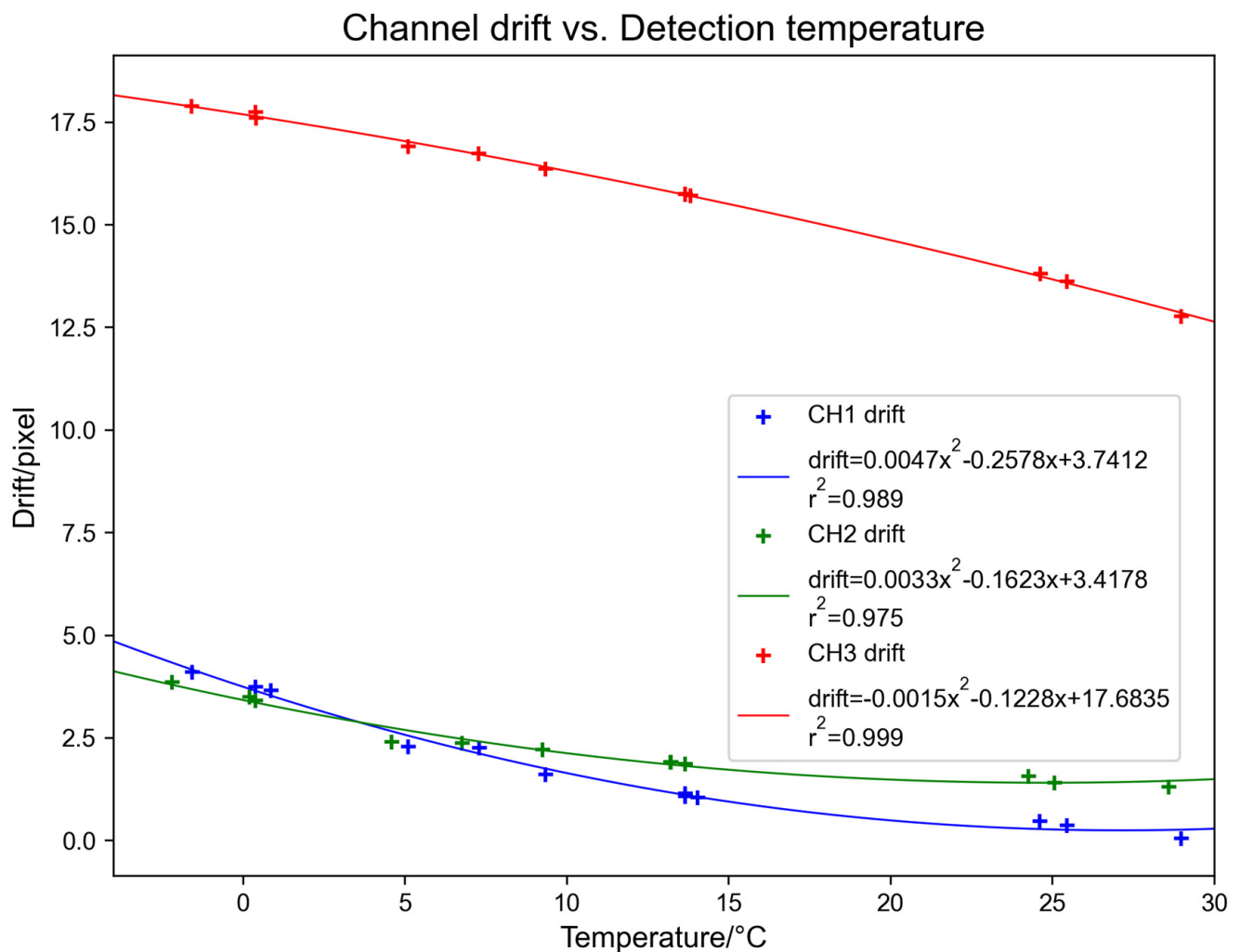


**Figure 6.** Fitting relationship of MarSCoDe spectral drift and CCD temperature: spectral drift and temperature are taken from the titanium target LIBS spectrum during Sol 32 to 92; the cross is the actual data point; and blue, green, and red solid lines represent the quadratic polynomial fitting curves of CH1, CH2, and CH3.

According to the MarSCoDe and ChemCam ground test results and the high correlation between the CCD temperature and the LIBS drift in each channel, we used a quadratic polynomial ( $\Delta x = a \times T^2 + b \times T + c$ ) to fit the CCD temperature and the value of the LIBS drift for each channel separately. The fitting results are shown in Table 2, and the goodness of fit  $r^2$  is above 0.95, indicating that the two follow a quadratic polynomial relationship. This relationship confirms that CCD temperature is the major factor resulting in wavelength drift. Other factors, such as the Martian environment and instrument jitter, may also exist,

but their effects are negligible. Additionally, it provides us with a wavelength calibration method that does not depend on data of a particular standard target taken in a specific LIBS observation.

**Table 2.** Parameters and goodness of fit obtained from quadratic polynomial fitting.

Channel	a	b	c	Quadratic Fitting $r^2$
CH1	0.0047	−0.2578	3.7412	0.989
CH2	0.0033	−0.1623	3.4178	0.975
CH3	−0.0015	−0.1228	17.6835	0.999

### 3. Results

According to the quadratic polynomial relationship obtained in Section 2.2.2, using the fit function, we can calculate the LIBS drift according to the temperature of the CCD when the LIBS data of each detection target are collected. Then the wavelength value of each pixel can be calibrated by substituting the drift as  $\Delta x$  into Equations (1)–(3). This method can be used for wavelength calibration in processing MarSCoDe LIBS data of both MCCT standard targets and Martian surface scientific targets. Due to the limited range of the data used in establishing the model, this calibration method is currently available when the CCD temperature is between  $-2$  and  $29$  °C.

In this section, we demonstrate the results of the Ti spectra of Sol 100, 103, and 110 calibrated by the method established above and the deviation of the calibrated wavelength relative to the actual value.

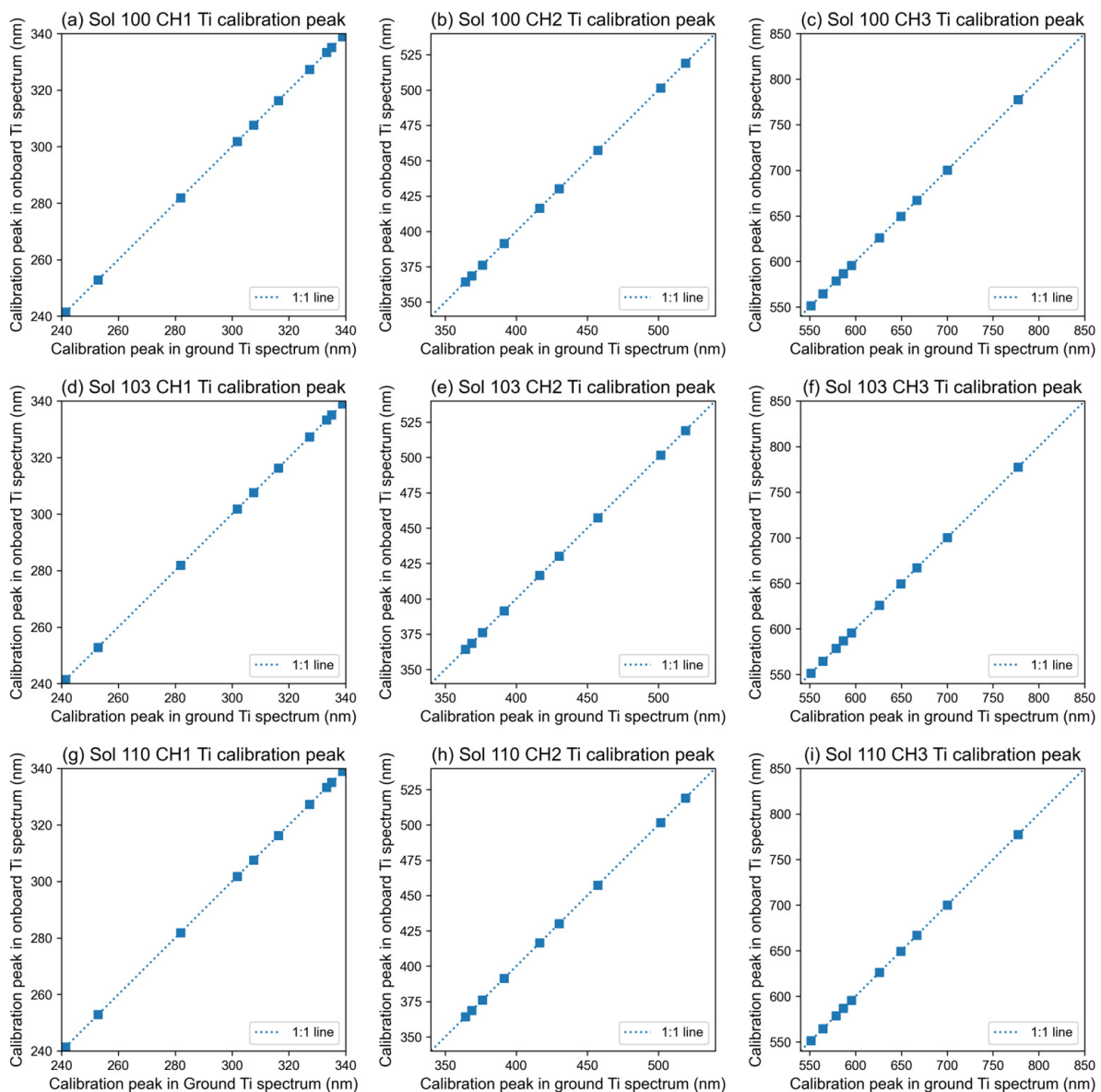
We counted the wavelength of calibration peaks calibrated by the method in this paper of the Ti plate mentioned above and the relative error and root mean square error of prediction (RMSEP) [16] of these peaks to these in reference spectra from the lab to evaluate the accuracy of this method. RMSEP shows the overall degree of deviation within a channel and is calculated according to Formula (4), where  $n$  is the number of emission peaks used in the spectrum, and  $d_i$  is the deviation between the calibrated wavelength of a certain calibration peak and the wavelength of the same one in the reference spectra from the lab:

$$\text{RMSEP} = \sqrt{\left(\sum_{i=1}^n d_i^2\right) / n} \quad (4)$$

The relative deviation maximum and RMSEP of Sol 100, 103, and 110 are shown in Table 3. The relative errors of the most drifted emission peaks of CH1, CH2, and CH3 are less than 0.013%, 0.010%, and 0.012%, which indicates that their deviations are negligible. RMSEP shows that the deviations of the calibrated wavelengths of CH1, CH2, and CH3 from the reference spectra from the lab are not more than 0.03, 0.03, and 0.05 nm, respectively, which are equivalent to 0.16, 0.01, and 0.11 of the spectral FWHM resolution of each channel and, therefore, are all less than 1/5 of the apparatus spectral width. This degree of deviation will not interfere with the LIBS analysis. Figure 7 shows a comparison of the wavelength of calibration peaks in the reference spectrum from the lab and in onboard spectra collected on Sol 100, 103, and 110.

**Table 3.** Drifts in Sol 100 to 110 titanium target LIBS spectra before calibration and their accuracy after wavelength calibration.

Sol	Channel	Drifts before Calibrated (nm)	Maximum Relative Error (%)	RMSEP (nm)
100	CH1	0.22	0.013	0.024
	CH2	0.39	0.008	0.022
	CH3	3.47	0.008	0.035
103	CH1	0.23	0.014	0.026
	CH2	0.41	0.010	0.027
	CH3	3.50	0.012	0.051
110	CH1	0.24	0.013	0.022
	CH2	0.43	0.010	0.030
	CH3	3.53	0.011	0.041

**Figure 7.** Comparison of calibration peak wavelengths of onboard spectra after calibration and reference spectrum from the lab. (a–c) show calibration peaks in CH1, CH2, and CH3 taken on Sol 100; (d–f) show calibration peaks in CH1, CH2, and CH3 taken on Sol 103; (g–i) show calibration peaks in CH1, CH2, and CH3 taken on Sol 110. Blue dotted lines are 1:1 lines.

The above results show that the LIBS wavelength calibration method established in this paper has good accuracy. The results processed by this method can provide an accurate wavelength for qualitative and quantitative analysis based on the LIBS spectrum taken by MarSCoDe.

#### 4. Discussion

In addition to the Ti plate, the application of the method to other emission peaks should also be discussed and evaluated. A comparison with the wavelength accuracy of similar payload data products is necessary to determine the method's effectiveness. The spectra of the norite target taken at Sol 41 and 43 were used to discuss the deviation of this method from the wavelength given by the NIST library and the corresponding emission peak wavelength values in the ChemCam norite data products. The norite standard target in MCCT was provided by France's Research Institute in Astrophysics and Planetology (IRAP), which is a duplicate of the ChemCam norite glass calibration target [19]. As of Sol 110, MarSCoDe has observed the norite target several times. LIBS data taken on the norite target on Sol 41 and 43 were processed by the method established in this paper. Results are compared with LIBS taken by ChemCam on the same target and evaluated based on the wavelength of these selected emission peaks recorded in the NIST spectral library. The wavelength of emission peaks in the NIST library is obtained from the C-QuEST tool [21].

We selected 20 representative emission lines of the major elements, including Mg, Na, Fe, Al, Ca, and Si, which are identified in the LIBS spectrum of the norite target taken by MarSCoDe on Sol 41 and 43 and by ChemCam on Sol 27. Results are shown in Figure 8. The deviation between the wavelength of these peaks in the LIBS spectrum and the standard wavelength provided by the NIST library is calculated. RMSEPs of the spectrum are also calculated according to Equation (4). Results are listed in Table 4 (see Table S3 in Supplementary Materials for detailed results).

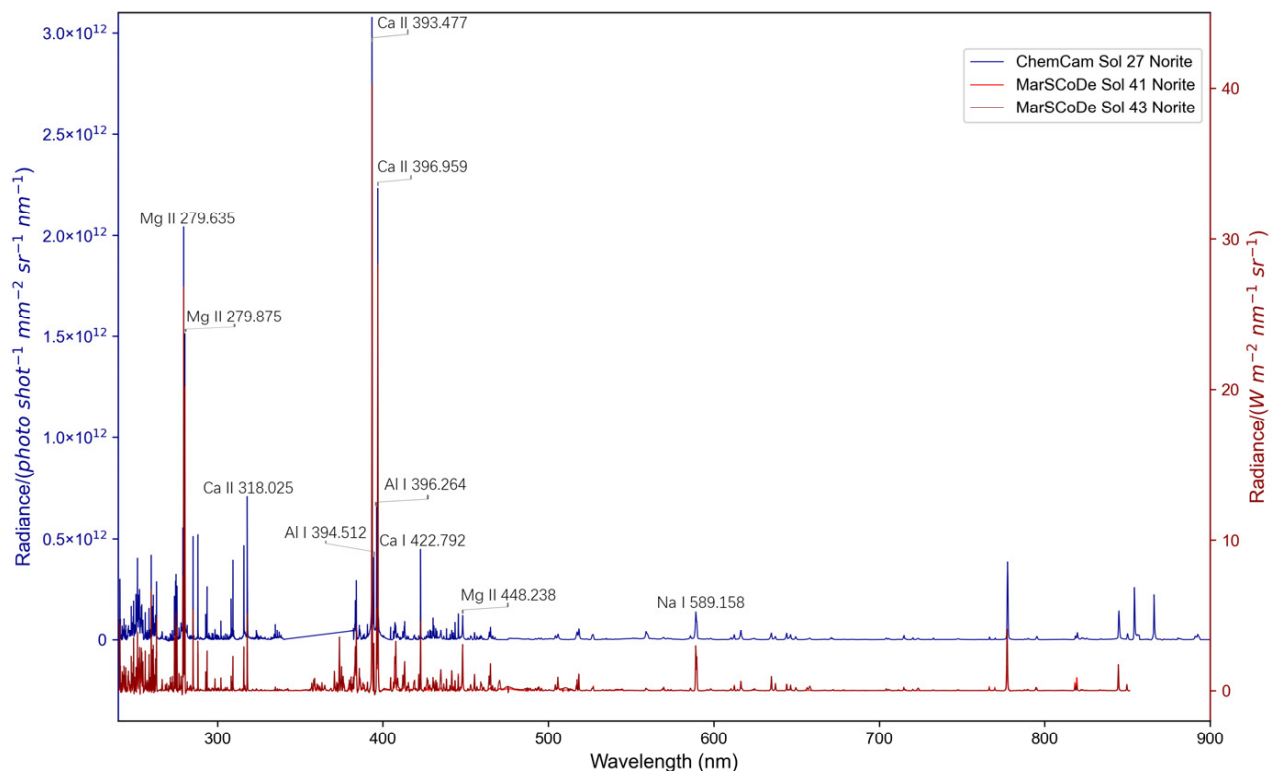


**Figure 8.** Comparison of the norite target LIBS spectrum taken by MarSCoDe on Sol 41 and 43 and ChemCam on Sol 27; part of the identified emission peaks is marked. ChemCam LIBS data could

be available at [https://pds-geosciences.wustl.edu/msl/msl-m-chemcam-libs-4\\_5-rdr-v1/mslccm\\_1xxx/data/](https://pds-geosciences.wustl.edu/msl/msl-m-chemcam-libs-4_5-rdr-v1/mslccm_1xxx/data/) (1 March 2022). To facilitate comparison and accurately identify the central wavelength of the emission peak, both MarSCoDe and ChemCam LIBS spectral data were resampled using the cubic spline function, and the spectral resolution after resampling was 0.001 nm.

The accuracies of ChemCam results and MarSCoDe calibrated by the method established in this paper are in the same order of magnitude according to Table 4, which proves that the calibration method established in this paper could provide an accurate wavelength for MarSCoDe LIBS data.

**Table 4.** Deviation of selected peaks in norite target LIBS spectrum taken by ChemCam and MarSCoDe from NIST.

Spectrum	Maximum Relative Error (%)	RMSEP (nm)
ChemCam Sol 27 Norite	0.012	0.017
MarSCoDe Sol 41 Norite	0.012	0.022
MarSCoDe Sol 43 Norite	0.014	0.025

## 5. Conclusions

We present a wavelength calibration method for MarSCoDe LIBS based on the quadratic function relationship between the drift of the MarSCoDe Ti plate LIBS spectrum relative to the reference spectra from the lab and the corresponding LIBS spectrometer CCD temperature. The relationship is found from the phenomenon that the CCD temperature of MarSCoDe LIBS increases with operating time due to the lack of active thermal control measures, and the drift of the same emission peak between different targets is inconsistent. In practice, the drift of the corresponding channel is calculated based on the CCD temperature of the in situ LIBS data, and the wavelength of the spectrum is then calibrated. The inspection of the subsequent LIBS data of the Ti plate showed that the overall deviation of the corrected wavelength values of each channel calibrated by this method relative to the reference spectra from the lab did not exceed 0.03, 0.03, and 0.05, which was enough to avoid the misjudgment in the identity of emission peaks. The inspection of the norite target shows that the accuracy of the calibrated wavelength of MarSCoDe LIBS is consistent with that of ChemCam. Due to the limitation of the data range of the established method, this method is currently suggested as available for CCD temperatures in the range of  $-2$  to  $29$  °C. When the CCD temperature of subsequent LIBS data appears outside this range, the same idea can be followed to modify the calibration method.

**Supplementary Materials:** The following supporting information can be downloaded at: <https://www.mdpi.com/article/10.3390/rs15061494/s1>, Table S1: Reference spectra from the lab of the Ti plate; Table S2: Details of calibration peaks; Table S3: Wavelengths and deviation of selected peaks in the spectra of the norite target collected by ChemCam and MarSCoDe.

**Author Contributions:** Conceptualization and writing—review and editing, X.R. and C.L.; methodology, Y.Z.; software, Y.Z. and Z.C.; validation, Y.Z. and Z.C.; formal analysis, Y.Z., Z.Z., X.L. and W.X.; investigation, Y.Z.; resources and data curation, W.C.; writing—original draft preparation, Y.Z.; visualization, Y.Z.; supervision, X.R., J.L. and C.L. All authors have read and agreed to the published version of the manuscript.

**Funding:** This study was funded by the Key Research Program of the Chinese Academy of Sciences (Grant No. ZDBS-SSW-TLC001).

**Data Availability Statement:** MarSCoDe LIBS data used in this study are available for download from the Lunar and Planetary Data Release System at <https://moon.bao.ac.cn/web/zhmanager/mars1#none> (accessed on 8 April 2022). All the data presented in this study are available on request from the corresponding author.

**Acknowledgments:** This work was supported by China National Space Administration (CNSA). We thank the team members of the five systems of the Tianwen-1 mission: the Probe System, the Launch Vehicle System, the Launch Site System, the Telemetry Track and Command System (TT&C), and the Ground Research and Application System (GRAS). We thank Lin Guo and Yuan Chen for their useful writing advice.

**Conflicts of Interest:** The authors declare no conflict of interest.

## References

1. Hahn, D.W.; Omenetto, N. Laser-Induced Breakdown Spectroscopy (LIBS), Part I: Review of Basic Diagnostics and Plasma-Particle Interactions: Still-Challenging Issues Within the Analytical Plasma Community. *Appl. Spectrosc.* **2010**, *64*, 335A–366A. [[CrossRef](#)] [[PubMed](#)]
2. Hahn, D.W.; Omenetto, N. Laser-induced breakdown spectroscopy (LIBS), part II: Review of instrumental and methodological approaches to material analysis and applications to different fields. *Appl. Spectrosc.* **2012**, *66*, 347–419. [[CrossRef](#)] [[PubMed](#)]
3. Cremers, D.A.; Radziemski, L.J. *Handbook of Laser-Induced Breakdown Spectroscopy*; John Wiley & Sons: Hoboken, NJ, USA, 2013. [[CrossRef](#)]
4. Wiens, R.C.; Maurice, S.; Barraclough, B.; Saccoccio, M.; Barkley, W.C.; Bell, J.F.; Bender, S.; Bernardin, J.; Blaney, D.; Blank, J.; et al. The ChemCam Instrument Suite on the Mars Science Laboratory (MSL) Rover: Body Unit and Combined System Tests. *Space Sci. Rev.* **2012**, *170*, 167–227. [[CrossRef](#)]
5. Maurice, S.; Wiens, R.C.; Saccoccio, M.; Barraclough, B.; Gasnault, O.; Forni, O.; Mangold, N.; Baratoux, D.; Bender, S.; Berger, G.; et al. The ChemCam Instrument Suite on the Mars Science Laboratory (MSL) Rover: Science Objectives and Mast Unit Description. *Space Sci. Rev.* **2012**, *170*, 95–166. [[CrossRef](#)]
6. Maurice, S.; Clegg, S.M.; Wiens, R.C.; Gasnault, O.; Rapin, W.; Forni, O.; Cousin, A.; Sautter, V.; Mangold, N.; Le Deit, L.; et al. ChemCam activities and discoveries during the nominal mission of the Mars Science Laboratory in Gale crater, Mars. *J. Anal. At. Spectrom.* **2016**, *31*, 863–889. [[CrossRef](#)]
7. Ehlmann, B.L.; Edgett, K.S.; Sutter, B.; Achilles, C.N.; Litvak, M.L.; Lapotre, M.G.A.; Sullivan, R.; Fraeman, A.A.; Arvidson, R.E.; Blake, D.F.; et al. Chemistry, mineralogy, and grain properties at Namib and High dunes, Bagnold dune field, Gale crater, Mars: A synthesis of Curiosity rover observations. *J. Geophys. Res. Planets* **2017**, *122*, 2510–2543. [[CrossRef](#)] [[PubMed](#)]
8. Cousin, A.; Dehouck, E.; Meslin, P.Y.; Forni, O.; Williams, A.J.; Stein, N.; Gasnault, O.; Bridges, N.; Ehlmann, B.; Schroder, S.; et al. Geochemistry of the Bagnold dune field as observed by ChemCam and comparison with other aeolian deposits at Gale Crater. *J. Geophys. Res. Planets* **2017**, *122*, 2144–2162. [[CrossRef](#)]
9. Lasue, J.; Cousin, A.; Meslin, P.Y.; Mangold, N.; Wiens, R.C.; Berger, G.; Dehouck, E.; Forni, O.; Goetz, W.; Gasnault, O.; et al. Martian Eolian Dust Probed by ChemCam. *Geophys. Res. Lett.* **2018**, *45*, 10968–10977. [[CrossRef](#)]
10. Thomas, N.H.; Ehlmann, B.L.; Meslin, P.Y.; Rapin, W.; Anderson, D.E.; Rivera-Hernandez, F.; Forni, O.; Schroder, S.; Cousin, A.; Mangold, N.; et al. Mars Science Laboratory Observations of Chloride Salts in Gale Crater, Mars. *Geophys. Res. Lett.* **2019**, *46*, 10754–10763. [[CrossRef](#)] [[PubMed](#)]
11. Thomas, N.H.; Ehlmann, B.L.; Anderson, D.E.; Clegg, S.M.; Forni, O.; Schroder, S.; Rapin, W.; Meslin, P.Y.; Lasue, J.; Delapp, D.M.; et al. Characterization of Hydrogen in Basaltic Materials with Laser-Induced Breakdown Spectroscopy (LIBS) for Application to MSL ChemCam Data. *J. Geophys. Res. Planets* **2018**, *123*, 1996–2021. [[CrossRef](#)]
12. Nachon, M.; Clegg, S.M.; Mangold, N.; Schroder, S.; Kah, L.C.; Dromart, G.; Ollila, A.; Johnson, J.R.; Oehler, D.Z.; Bridges, J.C.; et al. Calcium sulfate veins characterized by ChemCam/Curiosity at Gale crater, Mars. *J. Geophys. Res. Planets* **2014**, *119*, 1991–2016. [[CrossRef](#)]
13. Anderson, D.E.; Ehlmann, B.L.; Forni, O.; Clegg, S.M.; Cousin, A.; Thomas, N.H.; Lasue, J.; Delapp, D.M.; McNroy, R.E.; Gasnault, O.; et al. Characterization of LIBS emission lines for the identification of chlorides, carbonates, and sulfates in salt/basalt mixtures for the application to MSL ChemCam data. *J. Geophys. Res. Planets* **2017**, *122*, 744–770. [[CrossRef](#)]
14. Wiens, R.C.; Maurice, S.; Robinson, S.H.; Nelson, A.E.; Cais, P.; Bernardi, P.; Newell, R.T.; Clegg, S.; Sharma, S.K.; Storms, S.; et al. The SuperCam Instrument Suite on the NASA Mars 2020 Rover: Body Unit and Combined System Tests. *Space Sci. Rev.* **2021**, *217*, 4. [[CrossRef](#)] [[PubMed](#)]
15. Maurice, S.; Wiens, R.C.; Bernardi, P.; Cais, P.; Robinson, S.; Nelson, T.; Gasnault, O.; Reess, J.M.; Deleuze, M.; Rull, F.; et al. The SuperCam Instrument Suite on the Mars 2020 Rover: Science Objectives and Mast-Unit Description. *Space Sci. Rev.* **2021**, *217*, 47. [[CrossRef](#)]
16. Wiens, R.C.; Maurice, S.; Lasue, J.; Forni, O.; Anderson, R.B.; Clegg, S.; Bender, S.; Blaney, D.; Barraclough, B.L.; Cousin, A.; et al. Pre-flight calibration and initial data processing for the ChemCam laser-induced breakdown spectroscopy instrument on the Mars Science Laboratory rover. *Spectrochim. Acta Part B At. Spectrosc.* **2013**, *82*, 1–27. [[CrossRef](#)]
17. Clegg, S.M.; Wiens, R.C.; Anderson, R.; Forni, O.; Frydenvang, J.; Lasue, J.; Cousin, A.; Payre, V.; Boucher, T.; Dyar, M.D.; et al. Recalibration of the Mars Science Laboratory ChemCam instrument with an expanded geochemical database. *Spectrochim. Acta Part B At. Spectrosc.* **2017**, *129*, 64–85. [[CrossRef](#)]
18. Xu, W.M.; Liu, X.F.; Yan, Z.X.; Li, L.N.; Zhang, Z.Q.; Kuang, Y.W.; Jiang, H.; Yu, H.X.; Yang, F.; Liu, C.F.; et al. The MarSCoDe Instrument Suite on the Mars Rover of China's Tianwen-1 Mission. *Space Sci. Rev.* **2021**, *217*, 64. [[CrossRef](#)]

19. Fabre, C.; Maurice, S.; Cousin, A.; Wiens, R.C.; Forni, O.; Sautter, V.; Guillaume, D. Onboard calibration igneous targets for the Mars Science Laboratory Curiosity rover and the Chemistry Camera laser induced breakdown spectroscopy instrument. *Spectrochim. Acta Part B At. Spectrosc.* **2011**, *66*, 280–289. [[CrossRef](#)]
20. Eilers, P.H. A perfect smoother. *Anal. Chem.* **2003**, *75*, 3631–3636. [[CrossRef](#)] [[PubMed](#)]
21. Cousin, A.; Forni, A.; Maurice, S.; Gasnault, O.; Fabre, C.; Sautter, V.; Wiens, R.C.; Mazoyer, J. Laser induced breakdown spectroscopy library for the Martian environment. *Spectrochim. Acta Part B At. Spectrosc.* **2011**, *66*, 805–814. [[CrossRef](#)]

**Disclaimer/Publisher’s Note:** The statements, opinions and data contained in all publications are solely those of the individual author(s) and contributor(s) and not of MDPI and/or the editor(s). MDPI and/or the editor(s) disclaim responsibility for any injury to people or property resulting from any ideas, methods, instructions or products referred to in the content.